

NFAT1 Transcription Factor Regulates Pulmonary Allergic Inflammation and Airway Responsiveness

Bruna P. F. Fonseca¹, Priscilla C. Olsen², Luciana P. Coelho², Tatiana P. T. Ferreira², Heitor S. Souza³, Marco A. Martins², and João P. B. Viola¹

¹Division of Cellular Biology, National Cancer Institute (INCA); ²Laboratory of Inflammation, Department of Physiology and Pharmacodynamics, Oswaldo Cruz Foundation (FIOCRUZ); and ³Multidisciplinary Laboratory, Clementino Fraga Filho University Hospital, Federal University of Rio de Janeiro (UFRJ), Rio de Janeiro, Brazil

Allergic asthma is a chronic inflammatory disease of the lung whose incidence and morbidity continues to rise in developed nations. Despite being a hallmark of asthma, the molecular mechanisms that determine airway hyperresponsiveness (AHR) are not completely established. Transcription factors of the NFAT family are involved in the regulation of several asthma-related genes. It has been shown that the absence of NFAT1 leads to an increased pleural eosinophilic allergic response accompanied by an increased production of Th2 cytokines, suggesting a role for NFAT1 in the regulation of allergic diseases. Herein, we analyze NFAT1^{-/-} mice to address the role of NFAT1 in a model of allergic airway inflammation and its influence in AHR. NFAT1^{-/-} mice submitted to airway inflammation display a significant exacerbation of several features of the allergic disease, including lung inflammation, eosinophilia, and serum IgE levels, which were concomitant with elevated Th2 cytokine production. However, in spite of the increased allergic phenotype, NFAT1^{-/-} mice failed to express AHR after methacholine aerosol. Refractoriness of NFAT1^{-/-} mice to methacholine was confirmed in naïve mice, suggesting that this refractoriness occurs in an intrinsic way, independent of the lung inflammation. In addition, NFAT1^{-/-} mice exhibit increased AHR in response to serotonin inhalation, suggesting a specific role for NFAT1 in the methacholine pathway of bronchoconstriction. Taken together, these data add support to the interpretation that NFAT1 acts as a counterregulatory mechanism to suppress allergic inflammation. Moreover, our findings suggest a novel role for NFAT1 protein in airway responsiveness mediated by the cholinergic pathway.

Keywords: allergic inflammation; asthma; NFAT; immune response; lung

Asthma is a chronic inflammatory disease of the lung that has been increasing in prevalence, morbidity, and mortality over the last two decades. The asthmatic disease has been closely associated with CD4 T helper (Th) 2 lymphocytes and correlated with pronounced levels of serum IgE, mast cell activation, and eosinophil recruitment and activation at the site of inflammation (1, 2). Airway hyperresponsiveness (AHR) is the physiologic cornerstone of this disease, being defined as an exaggerated bronchospastic response to nonspecific agonists, such as methacholine or serotonin, or specific antigens (3). AHR affects nearly 10% of the population in industrialized countries, and although many components of airway inflammation are associated with its

CLINICAL RELEVANCE

In this article, we address the involvement of NFAT1 in asthma. Although NFAT1^{-/-} mice display an exacerbation of pulmonary inflammation, they fail to express airway responsiveness to methacholine, suggesting a role for NFAT1 in regulating airway responsiveness.

development, the specific mechanisms by which AHR develops remains controversial. Many studies attempted to elucidate the molecular mechanisms that induce and/or maintain asthma and AHR, to provide insight for the design of new treatments for chronic lung diseases.

Over the past few years, the proteins of the NFAT (Nuclear Factor of Activated T cells) family of transcription factors have emerged as important players in the induction and development of allergic responses. The NFAT family of transcription factors encodes four distinct proteins that are regulated by the calcium/calcineurin signaling pathway, known as NFAT1 (also called NFATp, NFATc2), NFAT2 (NFATc, NFATc1), NFAT3 (NFATc4), NFAT4 (NFATx, NFATc3), and another protein named NFAT5 (TonE-BP), which is regulated by hyperosmotic stress (4, 5). NFAT proteins are expressed in a variety of cell types, including T cells, B cells, mast cells, natural killer cells, and eosinophils (4, 6), where they are activated by stimulation of calcium-mobilizing antigens and Fc receptors (4). In fact, proteins belonging to the NFAT family of transcription factors are well known for controlling the expression of many genes involved in the development of allergic responses (4). Binding sites for NFAT proteins have been described in the promoter/enhancer regions of some asthma-related genes, such as the IL-4, IL-5, and IL-13 encoding genes (4). These data suggest that deficiencies in NFAT1 protein may lead to the development of allergic diseases.

The disruption of the NFAT1-encoding gene has offered considerable evidence supporting a role for this transcription factor in the regulation of allergic diseases. It has been shown that NFAT1-deficient mice (NFAT1^{-/-}) develop an increased allergic response in a model of pleural inflammation, when compared with NFAT1^{+/+} mice (7, 8). The loss of NFAT1 protein leads to a marked increase in the number of eosinophils in the pleural cavity and a corresponding increase in serum IgE levels (7). This hypereosinophilic phenotype was also accompanied by increased IL-5 and IL-13 levels in the site of inflammation, suggesting that NFAT1^{-/-} mice are prone to develop a classically allergic phenotype (8). Consistently, NFAT1^{-/-} lymphocytes preferentially differentiate toward a Th2 phenotype, characterized by high levels of IL-4, IL-5, and IL-13 production, and confirmed by increased susceptibility of these mice to

(Received in original form March 21, 2007 and in final form May 16, 2008)

This work was supported by grants from CNPq (to J.P.B.V. and M.A.M.). B.P.F.F. was supported by a fellowship from the Brazilian Ministry of Health; P.C.O., L.P.C., and T.P.T.F. were supported by a fellowship from FAPERJ.

Correspondence and requests for reprints should be addressed to João P.B. Viola, M.D., Ph.D., Divisão de Biologia Celular, Instituto Nacional de Câncer, Rua André Cavalcanti 37, Rio de Janeiro 20231-050, Brasil. E-mail: jpviola@inca.gov.br

Am J Respir Cell Mol Biol Vol 40, pp 66–75, 2009

Originally Published in Press as DOI: 10.1165/rcmb.2007-01020C on July 29, 2008

Internet address: www.atsjournals.org

Leishmania major infection (9, 10). In addition, mice lacking NFAT4 have normal cytokine production, but NFAT1^{-/-} × NFAT4^{-/-} double knockout mice spontaneously develop a Th2-prevailing syndrome, illustrated by allergic blepharitis and interstitial pneumonitis (11). These features were accompanied by a striking increase in Th2 cytokines and resulted in markedly increased levels of the IL-4-dependent isotypes IgG1 and IgE in the sera of unimmunized mice (11). In spite of the data related to NFAT-deficient animals, a recent study with dominant-negative NFAT-transgenic mice submitted to an asthma experimental model has shown otherwise (12). Diehl and colleagues show that inhibition of all NFAT family members specifically in T cells impairs the development of a Th2 immune response *in vivo* and delay the lung eosinophil accumulation (12). These mice were also more resistant to the development of lung pathology associated with allergic airway inflammation in response to allergen exposure (12). It is important to note that the dominant-negative NFAT-transgenic mice present an inhibition of NFAT1–4 proteins activation.

Even though the elucidation of the specific roles of individual NFAT family members is quite challenging because of overlapping expression patterns of different members, inhibition of all NFAT family members goes against the idea that the five different proteins have distinct properties in the regulation of cytokine genes. All five NFAT members play specific roles during immune responses *in vivo*, and their effects on immune responses have to be considered separately. Therefore, our goal in this study was to address the role of one specific NFAT family member, NFAT1, in a model of a clinically relevant lung airway inflammation, a fact that has never been reported. In addition, for the first time, we show NFAT1 influence in one of the most important hallmarks of asthmatic disease, AHR. In this article, we provide evidence of a role for NFAT1 in modulating allergic responses, and describe a putative role for NFAT1 in mediating methacholine-evoked AHR.

MATERIALS AND METHODS

Animals, Cells, and Reagents

NFAT1^{+/+} and NFAT1^{-/-} (C57BL/6 × 129/Sv) 8- to 12-week-old female mice were used in all experiments (7). Animals were bred and maintained in the Brazilian National Cancer Institute animal facility. Animals were treated according to the guide for the care and use of laboratory animals (National Institutes of Health, Bethesda, MD). All primary cells (total lymphocytes) were cultured in Dulbecco's modified Eagle's medium supplemented with 10% fetal calf serum (FCS), L-glutamine, streptomycin-penicillin, essential and nonessential amino acids, sodium pyruvate, vitamins, and 2-mercapto-ethanol (all from Invitrogen, Carlsbad, CA). The 2C11 hybridoma (anti-CD3) was cultured in RPMI 1640 supplemented with 10% FCS. The Abs were purified from hybridoma supernatants by chromatography over protein G (Amersham Biosciences, Piscataway, NJ), and their activity was functionally tested by cellular proliferation and complement-dependent depletion. The immunosuppressive drug cyclosporin A (CsA) was obtained from Novartis (São Paulo, Brazil). The alum (aluminum hydroxide), complete Freund's Adjuvant (CFA), ovalbumin (OVA), methacholine chloride, serotonin (5-hydroxytryptamine), and carbachol were purchased from Sigma-Aldrich (St. Louis, MO). The solutions of May-Grünwald and Giemsa were obtained from Merck (Darmstadt, Germany).

Antigen-Induced Allergic Airway Disease Model

Naïve mice were immunized subcutaneously in one of the hind footpads with 50 µg of OVA emulsified in CFA. Seven days after the immunization, the sensitized mice received an intraperitoneal injection of 50 µg of OVA, in the absence of adjuvant. Seven days later, mice were challenged once a day for three consecutive days with aerosolized OVA (2.5%) dissolved in PBS through a nebulizer for 30 minutes. As

a control, PBS alone was administered through the nebulizer. The analyses were performed 24 hours after the last inhalation. Alternatively, naïve mice were immunized and challenged as described by Lloyd and coworkers (13). Briefly, mice were immunized intraperitoneally with 10 µg of OVA in 0.2 ml alum on Day 0. Then, mice were challenged intraperitoneally on Day 10 with 10 µg of OVA in 0.2 ml alum and daily between Days 19 and 24 with aerosolized 5% OVA for 20 minutes.

Bronchoalveolar Lavage

Mice were killed by carbon dioxide inhalation and their lungs underwent lavage twice with 0.5 ml cold PBS with 0.1% bovine serum albumin (BSA) (Sigma) via a polyethylene catheter (OD, 0.7 mm). The bronchoalveolar lavage (BAL) fluid was centrifuged and the cell pellets were resuspended in 0.5 ml of cold PBS with 0.1% BSA. Cells were counted, cytocentrifuged, and stained with May-Grünwald/Giemsa. At least 200 cells per slide were examined under light microscopy and characterized as neutrophils, mononuclear cells, or eosinophils, according to morphologic criteria.

Serum IgE Analysis

Blood samples of naïve and OVA-sensitized mice were collected by cardiac puncture. Serum was obtained by centrifugation of coagulated blood and assessed for IgE levels by enzyme-linked immunosorbent assay (ELISA) according to the manufacturer's instructions (BD PharMingen, San Diego, CA).

Lung Cytokine, Chemokine, and Lipid Mediator Measurements

A sagittal block of the left lung (0.1 g) was excised and placed in 1.0 ml of homogenization buffer (500 mM NaCl, 50 mM Hepes, pH 7.4, containing 0.1% Triton X-100, 0.5 mg/ml leupeptin, 1 mM PMSF, and 0.02% NaN₃). Lung tissues were individually homogenized with a tissue tearer, and processed as described previously (14). The resultant cleared supernatants were collected and used for measurement of total proteins and assessed for IL-13 and Eotaxin levels by ELISA (R&D Systems, Minneapolis, MN; BD PharMingen) and for Cys-Leucotriens (LTs) by EIA (Cayman Chemical Co., Ann Arbor, MI), according to the manufacturer's instructions.

Lung Histology

Lungs were inflated by injecting 1.0 ml of 10% buffered formalin through the catheter used to perform BAL. Lungs were then removed, fixed in the same solution, and embedded in paraffin. Lung sections (5 µm thick) were stained with hematoxylin and eosin (H&E), Gomori's trichrome, and periodic acid-Schiff (PAS) according to standard protocols and examined microscopically. Quantitative analysis of tissue sections and of captured images was performed by using a computer-assisted image analyzer (Image-Pro Plus Version 4.1 for Windows; Media Cybernetics, LP, Silver Spring, MD). One observer who was unaware of the experimental setting examined all tissue sections in a random fashion. Digital photographs of at least five bronchovascular bundles per tissue section (with bronchioles cross-sectional diameters ranging from 120 to 250 µm) were obtained under light microscopy at ×400 magnification. The Gomori's trichrome dye was used to stain collagen fibers in tissue. Density of collagen fibers was defined by the area positively stained for collagen in relation to total tissue in the area of the bronchovascular bundles per square millimeter. Mucus secretion from goblet cells of the bronchial epithelium was quantified by differential staining of sections with PAS. Goblet cells were recognized by their characteristic distended lateral border, basal nucleus, and the intense red staining of their content of mucus glycosaminoglycans with PAS. Numbers of goblet cells were expressed as the percentage of positive cells in at least 500 cells of the bronchial epithelium.

In Vitro Stimulation

Mice were immunized as described above. Fifteen days after sensitization, the draining lymph nodes (popliteal and inguinal) were harvested, and cells (2 × 10⁶ cells) were stimulated *in vitro* for 48 hours with plate-bound anti-CD3 (1 µg/ml). Cell-free supernatants were then assessed for IFN-γ and IL-4 by ELISA, according to the manufacturer's instructions (BD PharMingen).

Determination of Airway Responsiveness

Mice were placed, conscious and unrestrained, in cylindrical Plexiglass plethysmograph single-chambers that were connected to a Buxco apparatus for analyzing barometric plethysmography (Buxco Electronics, Sharon, CT). Mice were challenged for 2 minutes by means of inhalation of aerosolized methacholine or serotonin in PBS, starting at a concentration of 6.25 mg/ml or 5 mg/ml, respectively. Airway responsiveness was expressed as enhanced pause (Penh), an indirect measurement that is correlated with airway resistance, impedance, and intrapleural pressure (15). Airway responsiveness measurements were made over a 5-minute period, starting 2 minutes after completion of exposure to the aerosolized agonists, and average Penh values for the 5-minute period were calculated. The procedure was then serially repeated with methacholine at concentrations of 12.5 and 25.0 mg/ml or serotonin at concentrations of 10.0 and 20.0 mg/ml. Baseline measurements of Penh were obtained by exposure to the vehicle (PBS). In antigen-induced Penh analysis, the respiratory parameters were measured shortly after OVA provocation, at indicated time points, without the addition of agonists.

Assessment of *In Vivo* Respiratory Mechanics

Airway responsiveness was assessed as a change in airway function after challenge with aerosolized methacholine via the airways. Mice were anesthetized with nembutal (60 mg/kg) and neuromuscular activity was blocked with bromide pancuronium (1 mg/kg). Tracheostomized mice were mechanically ventilated and lung function was assessed 24 hours after the last antigen challenge. The trachea was cannulated and the cannula connected to a pneumotachograph. Air flow and transpulmonary pressure were recorded with a Buxco Pulmonary Mechanics Computer (Buxco Electronics). The computer calculated resistance (cm H₂O/ml/s) and dynamic lung compliance (ml/cm H₂O) in each breath cycle. Analog signals from the computer were digitized by a Buxco Analog converter. Animals were allowed to stabilize for 5 minutes and increasing concentrations of methacholine (3; 12.5; 25; 50 and 100 mg/ml) were aerosolized for 5 minutes each. Baseline pulmonary parameters were assessed with aerosolized PBS.

RT-PCR

For RT-PCR studies, lung slices of naïve mice were excised and immediately frozen in liquid nitrogen. Frozen tissue extracts were placed separately in 1.0 ml of TRIzol reagent (Invitrogen Life Technologies) and homogenized with a tissue tearor. Total RNA was then extracted and semiquantitative RT-PCR for the analysis of the expression of murine M₁, M₂, and M₃ mAChRs was performed as described previously (16). The primers used were as follows: M₁, 5'-CAG TCC CAA CAT CAC CGT CTT-3' and 5'-GAG AAC GAA GGA AAC CAA CCA C-3' (441-bp product); M₂, 5'-TGT CTC CCA GTC TAG TGC AAG G-3' and 5'-CAT TCT GAC CTG ACG ATC CAA C-3' (369-bp product); M₃, 5'-GTA CAA CCT CGC CTT TGT TTC C-3' and 5'-GAC AAG GAT GTT GCC GAT GAT G-3' (245-bp product); and GAPDH, 5'-GTG ATG GGT GTG AAC CAC GAG-3' and 5'-CCA CTA TGC CAA AGT TGT CA-3' (120-bp product). PCR conditions were as follows: 95°C for 10 minutes; 30 cycles at 94°C for 30 seconds, 62°C for 20 seconds, and 73°C for 30 seconds; and final elongation at 73°C for 7 minutes. PCR products were resolved on 1.5% agarose gels and visualized with ethidium bromide.

Tracheal Smooth Muscle Contraction

Isometric force measurements of tracheal smooth muscle contractility were determined in isolated tracheal rings preparations placed in aerated (95% O₂/5% CO₂) Krebs buffer (glucose 11 mM, NaCl 118 mM, CaCl₂ 2.5 mM, MgSO₄ 1.2 mM, KH₂PO₄ 1.2 mM, NaHCO₃ 24 mM) kept at 37°C. Tissues were allowed to equilibrate for 60 minutes under isometric tension of 1 g. At the end of the equilibration period, the tracheas were initially challenged with carbachol (5 × 10⁻⁶ M) to confirm viability of the preparation. After washout of carbachol and reestablishment of stable baseline tone, concentration dependency curves were constructed with the cumulative addition, at intervals of 1 minute, of either metacholine (10⁻⁸ to 10⁻⁴ M) or serotonin (10⁻⁸ to 3 × 10⁻⁵ M). All responses were expressed as percentage of response to 5.0 μM carbachol. Stimulation-induced isometric contractile responses were measured with a force-displacement transducer (Ugo Basile, Comerio,

Italy) and processed by an Isolated Organ Data Acquisition software (Proto 5; Letica Scientific Instruments, Barcelona, Spain).

Statistical Analysis

Statistical analysis of values from wild type (+/+) and knockout (-/-) mice and between control and treated groups was performed using unpaired Student's *t* test for single comparisons, or one-way ANOVA followed by Student-Newman-Keuls analysis for multiple comparisons. A value of *P* < 0.05 was considered statistically significant.

RESULTS

Exacerbated Allergic Inflammation in the Lungs of NFAT1^{-/-} Mice

To address the role of NFAT1 in the regulation of allergic airway inflammation, we examined the cardinal features of lung inflammation in NFAT1 wild-type (+/+) and knockout (-/-) allergen-sensitized and -challenged mice. As shown in Figure 1, after OVA inhalation the numbers of total cells and eosinophils in the BAL fluid of OVA-sensitized NFAT1^{-/-} mice were markedly increased when compared with OVA-sensitized NFAT1^{+/+} mice. This hypereosinophilic phenotype was accompanied by an increased IgE production in NFAT1^{-/-} mice when compared with NFAT1^{+/+} mice (Figure 2A), corroborating previous results shown by Viola and colleagues (8) in a pleurisy model.

As the pathophysiologic manifestations of allergic asthma are typically accompanied by robust Th2 immune responses, we next examined the pattern of cytokine production generated by

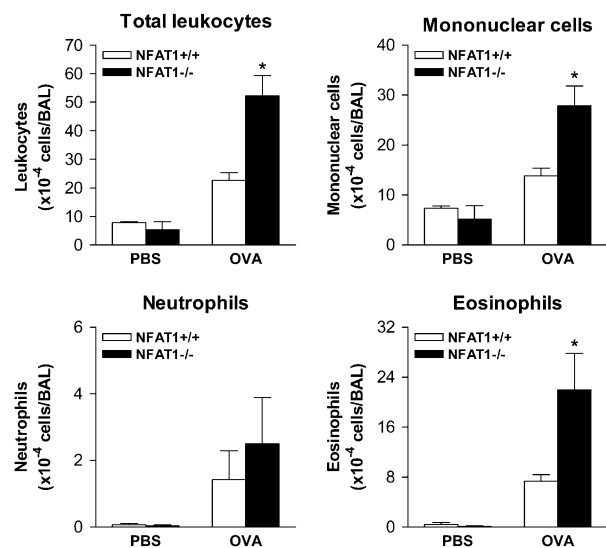


Figure 1. Increased lung eosinophilia in NFAT1^{-/-} mice after ovalbumin (OVA) sensitization and challenge. NFAT1^{+/+} and NFAT1^{-/-} mice were sensitized subcutaneously with OVA emulsified in CFA in a hind footpad. Seven days after sensitization, mice were sensitized intraperitoneally with OVA, without the presence of adjuvant. Seven days later, mice were challenged by the exposure of PBS or OVA aerosol for three consecutive days. The recovery of bronchoalveolar lavage (BAL) fluid cells was made 24 hours after the last day of challenge. BAL fluid cells were cytocentrifuged and counterstained with May-Grünwald/Giemsa for differential leukocyte analysis. Total numbers of lung total leukocytes, mononuclear cells, neutrophils, and eosinophils are shown in control (PBS) and treated (OVA) groups. Data are expressed as mean ± SEM (*n* = 5) and are representative of four independent experiments. *Significantly different values relative to OVA-challenged NFAT1^{+/+} mice (*P* < 0.05).

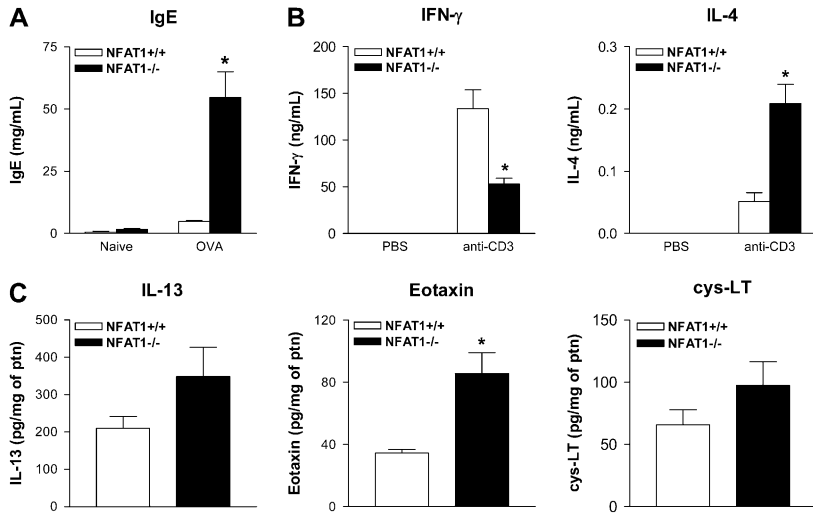


Figure 2. Increased IgE production, Th2 phenotype, and inflammatory mediator release in NFAT1^{-/-} mice. (A and C) Mice were sensitized and challenged as described in Figure 1. The analyses were made 24 hours after the last day of challenge. (A) Blood samples were collected by cardiac puncture of naïve and OVA-sensitized mice. Serum was obtained by centrifugation of coagulated blood and assessed for IgE levels by enzyme-linked immunosorbent assay (ELISA). (B) NFAT1^{+/+} and NFAT1^{-/-} mice were sensitized subcutaneously with OVA emulsified in CFA in a hind footpad. Seven days after sensitization, mice were sensitized intraperitoneally with OVA, without the presence of adjuvant. Seven days later, the draining lymph nodes of OVA-sensitized mice were harvested and the cells were stimulated *in vitro* with plate-bound anti-CD3 for 48 hours. Cell supernatants were then harvested and assessed for IFN-γ and IL-4 by ELISA. (C) Lungs were isolated, homogenized with a tissue tearor, and centrifuged. The supernatant was collected and assessed for IL-13 and eotaxin by ELISA and for cys-LT by EIA. Data are expressed as mean ± SEM (n = 5) and are representative of two independent experiments. *Significantly different values relative to NFAT1^{+/+} mice (P < 0.05).

for cys-LT by EIA. Data are expressed as mean ± SEM (n = 5) and are representative of two independent experiments. *Significantly different values relative to NFAT1^{+/+} mice (P < 0.05).

the OVA immune response. To evaluate the prevailing Th phenotype of OVA-sensitized mice, we examined anti-CD3-stimulated cytokine production in total lymph node cell cultures. As shown in Figure 2B, NFAT1^{-/-} mice presented an enhanced Th2 phenotype, characterized by higher levels of IL-4 production and lower levels of IFN-γ when compared with wild-type mice. It is worth pointing out that the increased Th2 phenotype seen in NFAT1^{-/-} mice cannot be attributed to differences in CD4 T cell numbers in the lymph nodes of NFAT1^{+/+} and NFAT1^{-/-} mice (NFAT1^{+/+}: 35% B cells, 35% CD4 T cells, and 30% CD8 T cells; NFAT1^{-/-}: 36% B cells, 36% CD4 T cells, and 28% CD8 T cells).

To measure the intensity of the allergic response in OVA-sensitized and -challenged mice, we examined the production of central allergic airway inflammation mediators in lung cell extracts. The levels of eotaxin were greatly increased in the

lungs of NFAT1^{-/-} mice, corroborating the hypereosinophilic phenotype presented by these mice (Figure 2C). Although there was also a clear tendency toward an elevation in IL-13 and cys-LTs levels in the lungs from OVA-challenged NFAT1^{-/-} mice, these values did not reach statistical significance (Figure 2C).

Lung sections revealed an increased leukocyte infiltration in OVA-challenged NFAT1^{-/-} mice when compared with control mice, which was seen in a smaller extent in NFAT1^{+/+} mice (Figure 3A, *H&E panel*). In contrast, the quantitative analysis of collagen fibers in the lung tissue, demonstrated equal amounts of OVA-induced collagen deposition in NFAT1^{-/-} and NFAT1^{+/+} mice (Figure 3B). Surprisingly, the evaluation of airway mucins showed a decreased number of mucus-producing cells in OVA-challenged NFAT1^{-/-} mice in relation to NFAT1^{+/+} mice (Figures 3A, *PAS panel*, and 3B).

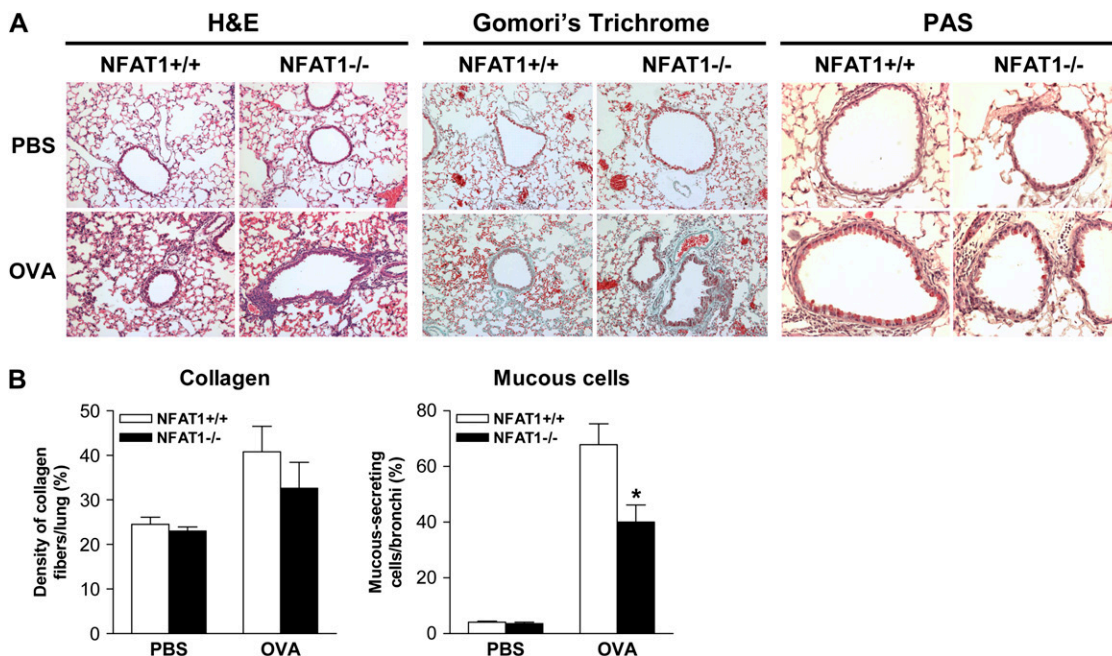


Figure 3. Characterization of NFAT1^{-/-} mice lung histology. (A and B) NFAT1^{+/+} and NFAT1^{-/-} mice were sensitized and challenged as described in Figure 1. Twenty-four hours after the last day of challenge, lungs were inflation-fixed in formalin 4%, embedded in paraffin, and sectioned. The tissue section slides were stained with hematoxylin and eosin (H&E), Gomori's Trichrome, or Periodic Acid Schiff (PAS). (A) Microscopic analysis of stained tissue sections. (B) Quantitative analysis of tissue sections stained with Gomori's

Trichrome and PAS. Data are representative of two independent experiments (n = 6). *Significantly different values relative to NFAT1^{+/+} mice (P < 0.05).

These results altogether clearly show that NFAT1^{-/-} mice, when submitted to experimentally induced allergic airway inflammation, develop an increased allergic response characterized by hyper eosinophilia and high serum IgE levels, besides presenting important asthma-like alterations in the lung tissue structure.

Involvement of NFAT1 in Methacholine-Induced Bronchoconstriction

The precise mechanisms that control AHR are poorly understood, but the magnitude of AHR has been closely associated with, among other factors, the degree of eosinophilic inflammation and airway remodeling (17, 18). Therefore, we addressed the airway responsiveness of NFAT1 wild-type and knockout mice using a selective muscarinic stimulus that causes bronchoconstriction, performing a dose-response curve by inhalation of methacholine. OVA sensitization and airway challenge led to the development of AHR in NFAT1^{+/+} mice, illustrated by significant increases in Penh values compared with PBS-challenged control mice (Figure 4A). In contrast, OVA-sensitized and -challenged NFAT1-deficient mice did not develop AHR even when exposed to higher methacholine concentrations, presenting Penh values similar to those of PBS-challenged control mice (Figure 4A).

To corroborate these results, we assessed the pulmonary mechanics of NFAT1^{+/+} and NFAT1^{-/-} OVA-sensitized and -challenged mice (Figure 4B). Lung function and methacholine responsiveness were measured in anesthetized, intubated, and mechanically ventilated mice. As shown in Figure 4B, there was a statistically significant decrease in lung resistance values in NFAT1^{-/-} mice when compared with NFAT1^{+/+} mice. Conversely, the analysis of airway compliance modulation did not reveal statically significant differences between NFAT1^{+/+} and NFAT1^{-/-} mice (Figure 4B). The reduction in respiratory resistance seen in NFAT1^{-/-} mice is consistent with the reduced baseline Penh as assessed by barometric plethysmography (Figure 4A).

To further analyze the decreased AHR response to methacholine observed in NFAT1^{-/-} mice, we evaluated the lung inflammation and pulmonary mechanics using another protocol to induce allergic airway inflammation. As shown in Figure 5A, NFAT1^{-/-} mice present increased numbers of total leukocytes and eosinophils in the BAL fluid after alum-OVA immunization and challenge when compared with NFAT1^{+/+} mice. However, although NFAT1^{-/-} mice present an enhanced infiltration of inflammatory cells in the lung upon OVA challenge, these mice still present a significant decrease in lung responsiveness to methacholine when compared with NFAT1^{+/+} mice (Figure 5B). In fact, there was an important decrease in lung resistance and an increase in compliance values of NFAT1^{-/-} mice in comparison with NFAT1^{+/+} mice (Figure 5B).

Altogether, the noninvasive barometric plethysmography results and invasive measurement of lung function confirmed NFAT1^{-/-} mice hyporesponsiveness to methacholine, strongly suggesting an involvement of NFAT1 in the modulation of methacholine-mediated bronchoconstriction. It is important to point out that these results demonstrate that the hyporesponsive phenotype observed in NFAT1^{-/-} mice is not due to adjuvant or route of antigen sensitization, since different protocols equally reproduce the phenotype seen in NFAT1^{-/-}.

Decreased Airway Hyperreactivity in NFAT1^{-/-} Mice Is Methacholine Specific

To further examine this phenomenon, we evaluated the methacholine-induced bronchoconstrictor response of naïve

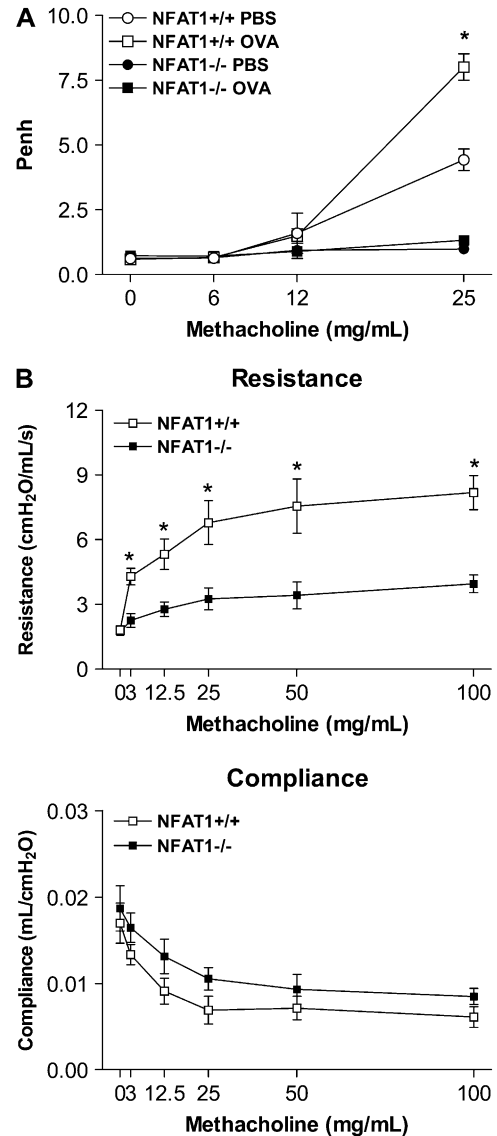


Figure 4. NFAT1^{-/-} mice develop decreased airway hyperresponsiveness (AHR) to methacholine. NFAT1^{+/+} and NFAT1^{-/-} mice were sensitized and challenged as described in Figure 1. The following analysis was made 24 hours after the last OVA challenge. (A) AHR to inhaled methacholine was measured using whole body barometric plethysmography. Penh was measured at baseline and after exposure to increasing concentrations of methacholine in OVA-sensitized and -challenged NFAT1^{+/+} and NFAT1^{-/-} mice. (B) Respiratory system resistance and compliance in response to increasing doses of methacholine in OVA-sensitized and -challenged mice. Data are expressed as mean \pm SEM ($n = 6$) and are representative of three independent experiments. *Significantly different values relative to OVA-challenged NFAT1^{+/+} mice ($P < 0.05$).

NFAT1^{+/+} and NFAT1^{-/-} mice. Consistent with the previous results, NFAT1^{-/-} naïve mice presented a decreased bronchoconstrictor response to methacholine when compared with NFAT1^{+/+} naïve mice (Figure 6A). These results show that NFAT1^{-/-} mice naturally have an impaired bronchoconstriction in response to methacholine, suggesting that NFAT1 could be involved in this process independently of the lung inflammatory status.

The activation of NFAT transcription factors requires sustained intracellular calcium (Ca^{2+}) levels, which activate the

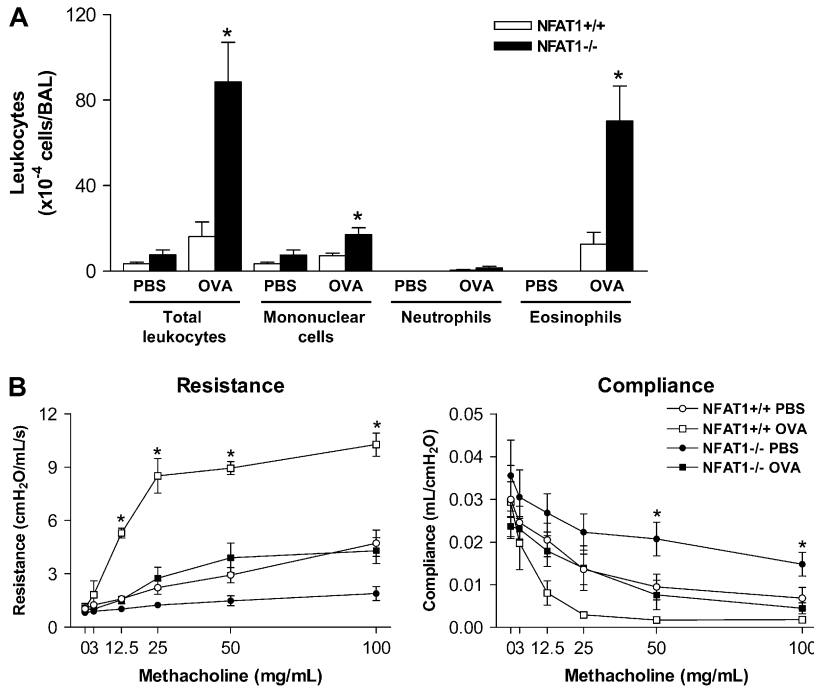


Figure 5. NFAT1^{-/-} mice hyporesponsiveness is independent of adjuvant and route of OVA sensitization. NFAT1^{+/+} and NFAT1^{-/-} mice were immunized intraperitoneally with OVA in alum on Day 0. Ten days later, mice were challenged intraperitoneally with OVA in alum, and then daily between Days 19 and 24 with OVA aerosol or PBS. (A) BAL fluid cells were cytocentrifuged and counterstained with May-Grünwald/Giemsa for differential leukocyte analysis. Total numbers of lung total leukocytes, mononuclear cells, neutrophils, and eosinophils are shown in control (PBS) and treated (OVA) groups. (B) Respiratory system resistance and compliance in response to increasing doses of methacholine in OVA-sensitized mice, challenged with PBS or OVA. Data are expressed as mean ± SEM (n = 6). *Significantly different values relative to OVA-challenged NFAT1^{+/+} mice (P < 0.05).

Ca²⁺-dependent phosphatase calcineurin. This process is blocked by the immunosuppressive drug CsA (4). To confirm the involvement of Ca²⁺-calcineurin pathway in methacholine-induced bronchoconstriction, we treated NFAT1^{+/+} naive mice with different doses of intraperitoneal CsA 3 hours before methacholine exposure. As shown in Figure 6B, CsA-treated NFAT1^{+/+} naive mice presented a dose-response inhibition of the methacholine-induced bronchoconstrictor response when compared with untreated control NFAT1^{+/+} mice, strongly suggesting a role of the involvement of Ca²⁺-calcineurin pathway in this phenomenon. Thus, inhibition of NFAT1 by CsA mimicked NFAT1^{-/-} phenotype, suggesting a role for NFAT1 in airway reactivity.

To determine whether the hyporesponsive phenotype of NFAT1^{-/-} mice was specific to cholinergic agonists, we examined responsivity to serotonin. As shown in Figure 6C, NFAT1^{+/+} and NFAT1^{-/-} naive mice presented similar Penh values when exposed to serotonin. In contrast, in OVA-sensitized and -challenged mice the absence of NFAT1 profoundly affected the degree of AHR after serotonin exposure. Thus, compared with NFAT1^{+/+} mice, NFAT1^{-/-} mice exhibited significantly increased AHR, illustrated by 2-fold higher Penh values observed at the highest serotonin concentration (Figure 6D). As serotonin is a noncholinergic agent, the increased responsiveness of NFAT1^{-/-} mice to serotonin strongly suggests a specific role for NFAT1 in the methacholine pathway of bronchoconstriction.

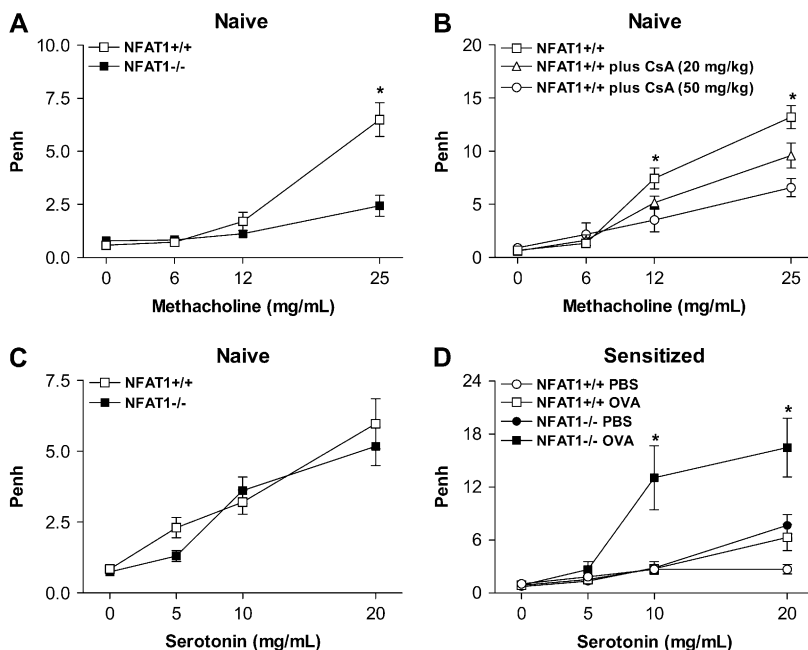


Figure 6. NFAT1^{-/-} mice hyporesponsiveness is methacholine specific. AHR to inhaled methacholine or serotonin was measured using whole body barometric plethysmography. Penh was measured at baseline and after sequential delivery of increasing concentrations of (A and B) methacholine or (C and D) serotonin, as indicated. (A and C) Analysis of naive NFAT1^{+/+} and NFAT1^{-/-} mice. (B) NFAT1^{+/+} naive mice were treated (intraperitoneally) with 20 mg/kg (open triangles) or 50 mg/kg (open circles) of ciclosporin A (CsA) and analyzed 3 hours after treatment. (D) NFAT1^{+/+} and NFAT1^{-/-} mice were sensitized and challenged as described in Figure 1. The following analysis was made 24 hours after the last OVA challenge. Data are expressed as mean ± SEM (n = 6) and are representative of three independent experiments. *Significantly different values relative to OVA-challenged NFAT1^{+/+} mice (P < 0.05).

NFAT1^{-/-} Mice Have Normal Expression of Muscarinic Receptors and Tracheal Smooth Muscle Contractility

Since M₃ mAChRs are the major receptors involved in airway bronchoconstriction mediated by the cholinergic pathway, we investigated whether the abrogation of the methacholine-induced bronchoconstrictor response seen in NFAT1^{-/-} mice could be explained by the impairment of mAChRs expression in the lung of these mice. We initially used a semiquantitative RT-PCR approach to evaluate the expression levels of M₁, M₂, and M₃ subtypes in total lung extracts of NFAT1^{+/+} and NFAT1^{-/-} naïve mice. As shown in Figure 7A, no differences were observed on mAChRs RNA expression levels in the lungs of NFAT1^{-/-} when compared with NFAT1^{+/+} mice.

We next assessed the functional activity of tracheal smooth muscle to rule out whether the inhibitory effect on bronchoconstriction seen in the absence of NFAT1 expression was mediated by differences in tracheal smooth muscle contractility. Isometric force measurements were analyzed by using isolated tracheas from NFAT1^{+/+} and NFAT1^{-/-} naïve and OVA-sensitized mice (Figure 7B). Using methacholine and serotonin as agonists, we observed no differences in contractile responses between the tracheas from NFAT1^{+/+} or NFAT1^{-/-} mice, represented by virtually superimposable concentration-response curves (Figure 7B). These results show that tracheal smooth muscle contractility and muscarinic receptor expression were not affected by NFAT1 deficiency, suggesting that the hyporesponsive phenotype observed in NFAT1^{-/-} mice cannot be due to alterations in tracheal smooth muscle contractile function.

DISCUSSION

The physiologic roles of NFAT1 in allergic responses are still largely unknown, hence we examined NFAT1-deficient mice in a model of a clinically relevant allergic disease such as allergic airway inflammation. The results described in this report revealed a major role for NFAT1 in modulating allergen-evoked lung inflammation, tissue remodeling, and airway hyperresponsiveness. There is considerable evidence supporting a role for NFAT1 in the regulation of allergic diseases. NFAT1^{-/-} mice submitted to a pleurisy model exhibit increased pleural eosinophilia and IgE serum levels (7, 8). These mice also presented increased levels of serum IgE in response to immunization with 2,4,6-trinitrophenol (TNP)-OVA (9). In line with these data, we report herein that NFAT1^{-/-} mice develop significantly increased allergic airway inflammatory response compared with NFAT1^{+/+} mice when immunized with OVA and then challenged by the same Ag through the airways. This exacerbated response was illustrated by a significantly higher degree of eosinophilic airway inflammation associated with increased IgE levels; increased IL-13, eotaxin, and cys-LTs

production; and augmented leukocyte infiltration in the lung tissue (Figures 1, 2, 3, and 5), all previously reported as cardinal features of asthma (1, 2, 18, 19). We also demonstrated the development of a Th2-biased immune response in NFAT1^{-/-} mice in comparison to NFAT1^{+/+} mice. These results are corroborated by previous data that show an increased production of Th2 cytokines by NFAT1^{-/-} lymph node cells, as well as a more efficient differentiation toward a Th2 phenotype in NFAT1^{-/-} spleen cells stimulated *in vitro* with IL-4 and anti-CD3 (8, 9). It has also been previously demonstrated that NFAT1^{-/-} lymphocytes preferentially differentiate toward a Th2 phenotype, observed both *in vitro*, in T cells stimulated with anti-CD3, and *in vivo*, in cells taken from the draining lymph nodes of mice injected several weeks before with *L. major* (10). These prior studies, along with the data presented in the present article, strongly suggest that alterations in NFAT1 proteins may result in altered gene expression and induction of allergic disorders.

In contrast, a recent study has shown that inhibition of all NFAT family members specifically in T cells prevents allergic pulmonary inflammation (12). In this study, the measurement of airway inflammation in mice was presented as a score related to different extents of leukocyte accumulation in the lung tissue subsequent to a model of lung allergic inflammation. Dominant-negative NFAT-transgenic mice exhibited a diminished inflammatory infiltrate in the lungs, despite normal levels of eosinophils in the BAL fluid when compared with wild-type mice (12). Although airway inflammation is often used as a marker of asthma, a better measure of asthma is AHR, which is generally considered to be one of the best objective clinical diagnostic tests for asthma (20–22). Consequently, studies of allergic airway inflammation, particularly in mice, should address AHR measures to arrive at accurate conclusions and/or correlations regarding human asthma. The results presented by Diehl and colleagues intended to bypass the effects of NFAT disruption in other tissues as well as altered expression of other NFAT family members caused by single NFAT protein deletions (12). However, it is worth pointing out that this family of transcription factors comprises five proteins with distinct properties of gene regulation in a variety of tissues, a fact that cannot be overlooked. The data observed in single NFAT-deficient mice support the idea that different NFAT family members may play specific roles during immune responses *in vivo*, and for that reason their functions should be considered separately.

AHR is an important feature of asthma and a major risk factor for accelerated decline of lung function in humans (23). In spite of its magnitude, the exact mechanism(s) underlying the development of AHR in chronic lung diseases such as asthma remains unknown. The analysis of the frequency of eosinophils present in the sputum of patients with asthma demonstrated a significant correlation between eosinophilia and AHR (24). In

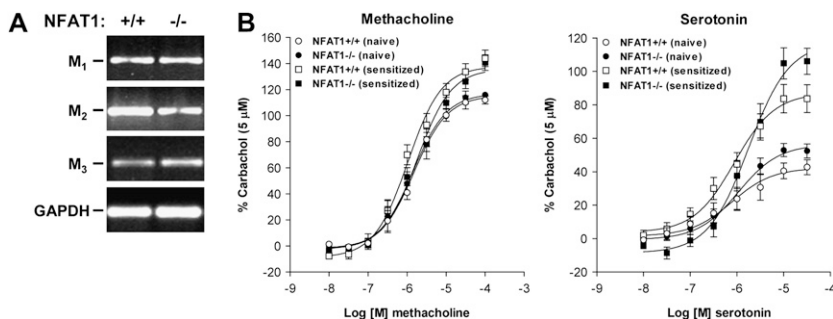


Figure 7. Normal expression of muscarinic receptors and tracheal contractility in NFAT1^{-/-} mice. (A) Primers specific for murine M₁, M₂, and M₃ muscarinic receptors were used to amplify cDNA derived from total RNA of lung tissue extracts of naïve NFAT1^{+/+} (left column) and NFAT1^{-/-} (right column) mice. Data are representative of three independent experiments ($n = 3$). (B) Stimulation-induced tension responses of isolated tracheas from NFAT1^{+/+} and NFAT1^{-/-} naïve and OVA-sensitized and -challenged mice, measured in the presence of increasing concentrations of methacholine (left graph) or serotonin (right graph), as

indicated. All responses were expressed as percentage of response to 5.0 μM carbachol. Data are expressed as mean ± SEM ($n = 4$) and are representative of three independent experiments.

addition, the severity of the asthmatic reaction has been associated to the number of activated T lymphocytes and eosinophils in BAL fluids of patients with asthma (25). The structural changes of the airway wall, collectively referred to as airway remodeling, have also been implicated in AHR (18). In humans, this phenomenon was evaluated through bronchoscopy and bronchial biopsy of patients with asthma, demonstrating a close correlation between the thickening of the basal membrane and functional severity of asthma (26). Together, our data indicate that functional disruption of NFAT1 leads to increases in a variety of asthmatic parameters and suggest that this transcription factor may be a critical regulator of allergic airway inflammation responses in mice.

Despite the exacerbation of the lung inflammation phenotype observed in NFAT1^{-/-} mice, these mice failed to respond to methacholine or to document AHR in response to inhaled methacholine, as shown in Figures 4A, 4B, and 5B. In addition to the results seen in immunized mice, NFAT1^{-/-} mice also present an intrinsically diminished methacholine-induced bronchoconstriction as observed in naïve mice (Figure 6A), which can be mimicked by CsA treatment in naïve NFAT1^{+/+} mice (Figure 6B). It is worth noting that this impairment in methacholine-induced bronchoconstriction observed in naïve NFAT1^{-/-} mice clearly demonstrates that this is an intrinsic effect, completely dissociated from the lung inflammatory status. In light of this finding, it seems unlikely that mechanisms induced by specific inflammatory mediators and/or infiltrating cells may be contributing to the methacholine-specific hyporesponsiveness seen in NFAT1^{-/-} mice. Alternatively, it has already been shown that the promoter region of the human M₃ mAChR gene has several NFAT-binding sites (27). Since this subtype is the main mAChR involved in airway bronchoconstriction, it would be logical to surmise that there might be significant changes in the number and/or function of M₃ mAChRs in the lungs of NFAT1^{-/-} mice. Our findings revealed, however, that NFAT1^{-/-} and NFAT1^{+/+} naïve mice exhibit comparable levels of M₁, M₂, and M₃ mAChRs expression, as attested by semiquantitative RT-PCR analysis of lung extracts (Figure 7A). In fact, previous studies have already shown that antigen challenge does not alter mAChR number, providing conclusive evidence that mAChR differential expression cannot be held responsible for airway responsiveness modulation *in vivo* (28, 29).

Because no significant change in the expression levels of the analyzed mAChRs was observed in the lungs of NFAT1^{-/-} mice, we hypothesized that a change in intracellular signaling via these receptors might be involved in the diminished bronchoconstriction seen in these mice. As mentioned previously, NFAT can be activated by mAChRs (30–32). When stimulated by ACh, M₁ and M₃ mAChRs generate an intracellular Ca²⁺ influx by activating the Phospholipase C (PLC) signaling cascade (33). Previous studies demonstrated that Jurkat T cells that ectopically express M₁ mAChR produce IL-2 and induce NFAT activity when stimulated with carbachol, a muscarinic agonist (30, 31). In addition, carbachol also induces robust luciferase responses in lymphoid and nonlymphoid cell lineages expressing an NFAT-luciferase reporter construct and an M₃ mAChR expression vector (32). This response is specific for the M₃ subtype of mAChRs and can be blocked by CsA in both lineages (33). Since NFAT1 is a transcription factor and bronchoconstriction an immediate process, we cannot discard the possibility that NFAT1 ablation results in aberrant expression of other developmentally regulated or physiologically relevant genes whose function may provide a direct mechanism for the diminished responsiveness to methacholine that we observed in NFAT1^{-/-} mice.

Cyclosporine A has been shown to improve lung function and decrease oral corticosteroid requirement in individuals with

chronic severe asthma and to inhibit the late-phase response after allergen challenge in individuals with mild atopic asthma (34–36). A recent work has also attributed CsA effects on the inhibition of airway inflammation and hyperresponsiveness to suppression of cytokines and inflammatory cells (37). Here we show that CsA also has a direct role in the inhibition of bronchoconstriction, mediating its effect independently of the lung inflammatory status, which suggests a role for the Ca²⁺-calcineurin pathway in bronchoconstriction. These data might seem conflicting at first for the fact that CsA inhibits NFAT members and yet inflammation is exaggerated in NFAT1^{-/-} mice. However, one has to consider the fact that CsA inhibits the activation of all NFAT1–4 proteins (4). It has been shown that mice deficient in either of these genes have markedly divergent phenotypes, suggesting that the individual NFAT proteins may play specific roles *in vivo*. In fact, data generated by gene disruption demonstrated that NFAT1 and NFAT2 proteins have opposite roles in Th differentiation *in vivo*. NFAT1^{-/-} mice showed an enhanced Th2 development as evidenced by increased levels of IL-4 production (9, 10). On the other hand, NFAT2^{-/-} lymphocytes displayed a decreased production of IL-4, demonstrating an impaired Th2 response (38). Our data demonstrated that naïve NFAT1^{+/+} treated with CsA presented the exact same phenotype observed in NFAT1^{-/-} mice, showing a decreased response to methacholine. These results suggest a role of the NFAT1 protein in bronchoconstriction in response to methacholine stimulation, which is independent of the enhanced lung allergic inflammation observed in NFAT1^{-/-} mice.

In spite of the increased allergic phenotype, OVA-challenged NFAT1^{-/-} mice also presented a diminished number of mucus-producing cells in the airways when compared with NFAT1^{+/+} mice, as shown in Figures 3A and 3B. The increased secretory response of mucus-producing cells is closely related to the effects of inflammatory mediators, particularly IL-13, and neural mechanisms, especially the ones of the cholinergic pathway (39). In fact, M₃ mAChRs are the predominant receptors mediating cholinergic-induced mucus secretion (40). The principal mucus-secreting cells of the airways are the surface epithelial goblet cells and the mucous cells of the submucosal glands (41). Submucosal glands express functional mAChRs M₁ and M₃, and goblet cells can also produce mucus in response to mAChRs stimulation (42). Once NFAT can be activated by M₁ and M₃ mAChRs (30–32), the absence of this transcription factor could compromise the induction of mucus secretion by these cells, in spite of IL-13 presence in the airways.

On the other hand, herein we demonstrate that NFAT1^{-/-} mice exhibit substantially enhanced AHR in response to serotonin inhalation when compared with NFAT1^{+/+} (Figure 6D). Serotonin induces bronchoconstriction in most mammalian species via G protein-coupled receptors, termed 5-HT₂ (43). Although it is well known that serotonin induced activation of 5-HT_{2A} receptors results in intracellular mobilization of Ca²⁺, similar to ACh, the exact mechanisms of serotonin-induced bronchoconstriction are to be defined (44). Although serotonin bronchoconstricting effects are traditionally interpreted as mediated via the cholinergic pathway (45, 46), several evidence have been emerging for an ACh-independent role of serotonin in mediating bronchoconstriction. Studies with lung slices showed no effects of atropine on serotonin-induced contraction of airways even though atropine completely blocked airway contraction induced by ACh (44). Recently, Kummer and coworkers have reported that 5-HT_{2A} receptors induce epithelium-dependent contractions, in an mAChR-unrelated manner, via a noncholinergic contractile factor, in addition to a direct stimulatory effect on the smooth muscle (47). Using video-

morphometric studies, the authors show that precision-cut lung slices from $M_2^{-/-} \times M_3^{-/-}$ double knockout mice remain fully responsive to serotonin, while no longer showing a bronchoconstrictor response after cholinergic stimulation (47). Altogether these data clearly indicate dissociation between serotonin and ACh constriction pathways, supporting the concomitant methacholine unresponsiveness and serotonin normoresponsiveness seen in NFAT1 $^{-/-}$ mice. The process of smooth muscle contractility is extremely complex and can be regulated by a variety of factors, some of which have already been shown to be altered in asthmatic airways (48). The assays with isolated tracheas showed in Figure 7B demonstrated no alterations in tracheal smooth muscle contractility, which could suggest that smooth muscle contractile function is preserved in NFAT1 $^{-/-}$ mice. However, previous studies have shown a distinct regional difference in smooth muscle responsiveness after repeated antigen challenge between tracheal and bronchial smooth muscle (29, 49). This regional difference in the development of smooth muscle hyperresponsiveness has been attributed to differences in the development of inflammation, alterations in antigen-induced changes in vascular permeability, and differences in neural control between tracheal and bronchial tissues (29, 50). In conclusion, our data are in line with the interpretation that NFAT1 acts as a counterregulatory mechanism to suppress lung allergic inflammation and reveal a novel role for NFAT1 protein in airway responsiveness mediated by the cholinergic pathway. However, additional analyses will be required to completely dissect the pathways involved in this NFAT1-dependent response.

Conflict of Interest Statement: None of the authors has a financial relationship with a commercial entity that has an interest in the subject of this manuscript.

Acknowledgments: The authors are especially grateful to Patricia T. Bozza for comments on the work and manuscript, and members of our laboratory for helpful advices and discussions. The authors are in debt to A. Rao for kindly providing the NFAT1 $^{-/-}$ mice, and to Ana Lucia de Aguiar Pires and Erika Azevedo for helping with the airway responsiveness experiments.

References

1. Renauld J-C. New insights into the role of cytokines in asthma. *J Clin Pathol* 2001;54:577-589.
2. Wills-Karp M. Immunologic basis of antigen-induced airway hyperresponsiveness. *Annu Rev Immunol* 1999;17:255-281.
3. Elias JA, Lee CG, Zheng T, Ma B, Homer RJ, Zhu Z. New insights into the pathogenesis of asthma. *J Clin Invest* 2003;111:291-297.
4. Rao A, Luo C, Hogan PG. Transcription factors of the NFAT family: regulation and function. *Annu Rev Immunol* 1997;15:707-747.
5. Lopez-Rodríguez C, Aramburu J, Rakeman AS, Rao A. NFAT5, a constitutively nuclear NFAT protein that does not cooperate with Fos and Jun. *Proc Natl Acad Sci USA* 1999;96:7214-7219.
6. Seminario MC, Guo J, Bochner BS, Beck LA, Georas SN. Human eosinophils constitutively express nuclear factor of activated T cells p and c. *J Allergy Clin Immunol* 2001;107:143-152.
7. Xanthoudakis S, Viola JP, Shaw KT, Luo C, Wallace JD, Bozza PT, Luk DC, Curran T, Rao A. An enhanced immune response in mice lacking the transcription factor NFAT1. *Science* 1996;272:892-895.
8. Viola JP, Kiani A, Bozza PT, Rao A. Regulation of allergic inflammation and eosinophil recruitment in mice lacking the transcription factor NFAT1: role of interleukin-4 (IL-4) and IL-5. *Blood* 1998;91:2223-2230.
9. Hodge RM, Ranger AM, De La Brousse FC, Hoey T, Grusby M, Glimcher L. Hyperproliferation and dysregulation of IL-4 expression in NF-ATp-deficient mice. *Immunity* 1996;4:397-405.
10. Kiani A, Viola JPB, Lichtman AH, Rao A. Down-regulation of IL-4 gene transcription and control of Th2 cell differentiation by a mechanism involving NFAT1. *Immunity* 1997;7:849-860.
11. Ranger AM, Oukka M, Rengarajan J, Glimcher LH. Inhibitory function of two NFAT family members in lymphoid homeostasis and Th2 development. *Immunity* 1998;9:627-635.
12. Diehl S, Krahl T, Rinaldi L, Norton R, Irvin CG, Rincon M. Inhibition of NFAT specifically in T cells prevents allergic pulmonary inflammation. *J Immunol* 2004;172:3597-3603.
13. Lloyd CM, Gonzalo JA, Nguyen T, Delaney T, Tian J, Oettgen H, Coyle AJ, Gutierrez-Ramos JC. Resolution of bronchial hyperresponsiveness and pulmonary inflammation is associated with IL-3 and tissue leukocyte apoptosis. *J Immunol* 2001;166:2033-2040.
14. Matsukawa A, Hogaboam CM, Lukacs NW, Lincoln PM, Strieter RM, Kunkel SL. Endogenous MCP-1 influences systemic cytokine balance in a murine model of acute septic peritonitis. *Exp Mol Pathol* 2000;68:77-84.
15. Hamelmann E, Schwarze J, Takeda K, Oshiba A, Larsen GL, Irvin CG, Gelfand EW. Noninvasive measurement of airway responsiveness in allergic mice using barometric plethysmography. *Am J Respir Crit Care Med* 1997;156:766-775.
16. Struckmann N, Schwering S, Wiegand S, Gschnell A, Yamada M, Kummer W, Wess J, Haberberger RV. Role of muscarinic receptor subtypes in the constriction of peripheral airways: studies on receptor-deficient mice. *Mol Pharmacol* 2003;64:1444-1451.
17. Jeffery PK, Wardlaw AJ, Nelson FC, Collins JV, Kay AB. Bronchial biopsies in asthma: an ultrastructural, quantitative study and correlation with hyperreactivity. *Am Rev Respir Dis* 1989;140:1745-1753.
18. Cohn L, Elias JA, Chupp GL. Asthma: mechanisms of disease persistence and progression. *Annu Rev Immunol* 2004;22:789-815.
19. Bradley BL, Azzawi M, Jacobson M, Assoufi B, Collins JV, Irani M, Schwartz LB, Durham SR, Jeffery PK, Kay AB. Eosinophils, T-lymphocytes, mast cells, neutrophils, and macrophages in bronchial biopsy specimens from atopic subjects with asthma: comparison with biopsy specimens from atopic subjects without asthma and normal control subjects and relationship to bronchial hyperresponsiveness. *J Allergy Clin Immunol* 1991;88:661-674.
20. Lewis SA, Weiss ST, Britton JR. Airway responsiveness and peak flow variability in the diagnosis of asthma for epidemiological studies. *Eur Respir J* 2001;18:921-927.
21. Ulrik CS, Postma DS, Backer V. Recognition of asthma in adolescents and young adults: which objective measure is best? *J Asthma* 2005;42:549-554.
22. Yurdakul AS, Dursun B, Canbakan S, Cakaloglu A, Capan N. The assessment of validity of different asthma diagnostic tools in adults. *J Asthma* 2005;42:843-846.
23. Lange P, Parner J, Vestbo J, Schnohr P, Jensen G. A 15-year follow-up study of ventilatory function in adults with asthma. *N Engl J Med* 1998;339:1194-1200.
24. Woodruff PG, Khashayar R, Lazarus SC, Janson S, Avila P, Boushey HA, Segal M, Fahy JV. Relationship between airway inflammation, hyperresponsiveness, and obstruction in asthma. *J Allergy Clin Immunol* 2001;108:753-758.
25. Walker C, Kaegi MK, Braun P, Blaser K. Activated T cells and eosinophilia in bronchoalveolar lavages from subjects with asthma correlated with disease severity. *J Allergy Clin Immunol* 1991;88:935-942.
26. Chetta A, Foresi A, Del Donno M, Bertorelli G, Pesci A, Olivieri D. Airways remodeling is a distinctive feature of asthma and is related to severity of disease. *Chest* 1997;111:852-857.
27. Forsythe SM, Kogut PC, McConville JF, Fu Y, McCauley JA, Halayko AJ, Liu HW, Kao A, Fernandes DJ, Bellam S, et al. Structure and transcription of the human m3 muscarinic receptor gene. *Am J Respir Cell Mol Biol* 2002;26:298-305.
28. Whicker SD, Compton MR, Seale JP, Black JL. Effect of sensitization and aerosol antigen challenge in guinea-pigs—studies of airway receptor function and characteristics. *Pulm Pharmacol* 1990;3:129-136.
29. Chiba Y, Ueno A, Sakai H, Misawa M. Hyperresponsiveness of bronchial but not tracheal smooth muscle in a murine model of allergic bronchial asthma. *Inflamm Res* 2004;53:636-642.
30. Desai DM, Newton ME, Kadlecck T, Weiss A. Stimulation of the phosphatidylinositol pathway can induce T-cell activation. *Nature* 1990;348:66-69.
31. Wu J, Katzav S, Weiss A. A functional T-cell receptor signaling pathway is required for p95vav activity. *Mol Cell Biol* 1995;15:4337-4346.
32. Boss V, Talpade DJ, Murphy TJ. Induction of NFAT-mediated transcription by Gq-coupled receptors in lymphoid and non-lymphoid cells. *J Biol Chem* 1996;271:10429-10432.
33. Felder C. Muscarinic acetylcholine receptors: signal transduction through multiple receptors. *FASEB J* 1995;9:619-625.
34. Alexander AG, Barnes NC, Kay AB. Cyclosporine A in corticosteroid-dependent chronic severe asthma. *Lancet* 1992;339:324-327.

35. Fukuda T, Asakawa J, Motojima S, Makino S. Cyclosporine A reduces T lymphocyte activity and improve airway hyperresponsiveness in corticosteroid-dependent chronic severe asthma. *Ann Allergy Asthma Immunol* 1995;75:65–72.
36. Khan LN, Kon ON, Macfarlane AJ, Meng Q, Ying S, Barnes NC, Kay AB. Attenuation of the allergen-induced late asthmatic reaction by cyclosporine A is associated with inhibition of bronchial eosinophils, interleukin-5, granulocyte macrophage colony-stimulating factor, and eotaxin. *Am J Respir Crit Care Med* 2000;162:1377–1382.
37. Lee YC, Kim SH, Seo YB, Roh SS, Lee JC. Inhibitory effects of *Actinidia polygama* extract and cyclosporine A on OVA-induced eosinophilia and bronchial hyperresponsiveness in a murine model of asthma. *Int Immunopharmacol* 2006;6:703–713.
38. Ranger AM, Hodge MR, Gravallese EM, Oukka M, Davidson L, Alt FW, Charles de la Brousse F, Hoey T, Grusby M, Glimcher LH. Delayed lymphoid repopulation with defects in IL-4-driven responses produced by inactivation of NF-ATc. *Immunity* 1998;8:125–134.
39. Rogers DF. Airway mucus hypersecretion in asthma: an undervalued pathology? *Curr Opin Pharmacol* 2004;4:241–250.
40. Bymaster FP, McKinzie DL, Felde CC, Wess J. Use of M₁–M₅ muscarinic receptor knockout mice as novel tools to delineate the physiological roles of the muscarinic cholinergic system. *Neurochem Res* 2003;28:437–442.
41. Rogers DF. Motor control of airway goblet cells and glands. *Respir Physiol* 2001;125:129–144.
42. Gosens R, Zaagsma J, Meurs H, Halayko AJ. Muscarinic receptor signaling in the pathophysiology of asthma and COPD. *Respir Res* 2006;7:73–88.
43. Hoyer D, Hannon JP, Martin GR. Molecular, pharmacological and functional diversity of 5-HT receptors. *Pharmacol Biochem Behav* 2002;71:533–554.
44. Perez JF, Sanderson MJ. The frequency of calcium oscillations induced by 5-HT, ACH, and KCl determine the contraction of smooth muscle cells of intrapulmonary bronchioles. *J Gen Physiol* 2005;125:535–553.
45. Eum SY, Norel X, Lefort J, Labat C, Vargaftig BB, Brink C. Anaphylactic bronchoconstriction in BP2 mice: interactions between serotonin and acetylcholine. *Br J Pharmacol* 1999;126:312–316.
46. Moffatt JD, Cocks TM, Page CP. Role of the epithelium and acetylcholine in mediating the contraction to 5-hydroxytryptamine in the mouse isolated trachea. *Br J Pharmacol* 2004;141:1159–1166.
47. Kummer W, Wiegand S, Akinci S, Wessler I, Schinkel AH, Wess J, Koepsell H, Haberberger RV, Lips KS. Role of acetylcholine and polyspecific cation transporters in serotonin-induced bronchoconstriction in the mouse. *Respir Res* 2006;7:65.
48. Stephens NL, Li W, Jiang H, Unruh H, Ma X. The biophysics of asthmatic airway smooth muscle. *Respir Physiol Neurobiol* 2003;137:125–140.
49. Misawa M, Chiba Y. Repeated antigenic challenge-induced airway hyperresponsiveness and airway inflammation in actively sensitized rats. *Jpn J Pharmacol* 1993;61:41–50.
50. Stretton D, Belvisi MG, Barnes PJ. The effect of sensory nerve depletion on cholinergic neurotransmission in guinea pig airways. *J Pharmacol Exp Ther* 1992;260:1073–1080.